

## HV bushing failure in service, diagnostics and modeling of oil-type bushings

Jacek Wańkowicz\* Jerzy Bielecki Marek Szrot Jan Subocz Ryszard Malewski  
Instytut Energetyki Energo-Complex ZUT Malewski Electric  
Poland  
[jacek.wankowicz@ien.com.pl](mailto:jacek.wankowicz@ien.com.pl)

### Introduction

Recently, a violent failure of HV bushing initiated fire that destroyed a large network transformer. A similar accident was reported on another transformer of the same age. A high cost of such failures prompted the utility to investigate the cause of bushings' explosion. The local manufacturer, who produced these transformers some thirty years ago, designed the internal insulation with a large safety margin. This generous safety margin increases their technical-life expectancy. However, 400 kV and 220 kV bushings were imported. These are oil-impregnated paper (OIP) bushings designed for approximately 30-year technical life, but no additional safety margin was provided. Most of these bushings are still in relatively good condition but their operational performance is difficult to predict in near future. Simultaneous replacement of all, nearly 400 bushings is impossible, considering their long delivery time and high cost. An effort was initiated to develop diagnostic procedures and a monitoring system to identify the bushings to be replaced first.

### Bushing failure mechanisms

An effective diagnostics shall be based on a known mechanism of insulation degradation, and two possible causes of bushing-insulation failure have been addressed in this report.

#### ■ Bushing failure due to moisture ingress through a leaky seal

One of them is due to penetration of atmospheric moisture into the bushing through aged sealing-gaskets, and gradual increase of water content in the bushing core. In such case the highest concentration of moisture is expected at the outer surface of the core.

#### ■ Incomplete moisture removal from the bushing-core inner-layer at the factory

Another possible cause is the manufacturing technology of oil-type bushings, which are heated in vacuum chamber to extract moisture trapped in thin paper layers separated by co-axial aluminum foils. The moisture is first evaporated from the paper layer edges, but if the vacuum is applied too fast then the evaporation becomes very intense. The latent heat of evaporation (enthalpy) is absorbed, and the temperature distribution along the bushing axis drops near the foils edge. That local temperature drop prevents an efficient extraction of moisture trapped in the middle section of the paper layers. In principle, the manufacturing technology requires a slow lowering of the pressure in the oven, and it may take a few weeks to dry 400 kV bushing.

An attempt to shorten this time results in leaving a wet-paper pocket usually near the bushing mid-length. Acceptance tests that involve measurements of capacitance and  $\tan \delta$  at power frequency do not reveal such small pocket of wet paper [1]. Such measurements indicate an average C- $\tan \delta$  of the whole stressed cellulose volume, and are not sensitive enough to detect a higher dielectric permittivity and loss of a relatively small volume of the wet paper.

## Investigation of failed 400 kV oil impregnated paper (OIP) transformer bushings

Luckily, some bushing failures were detected in time to prevent explosion and fire. Such units have been disassembled and examined for the mechanism of their insulation failure.



Fig.2. 400 kV transformer bushing type OIP that failed after some 30 years of service.

Once the porcelain housing was removed and the bushing core exposed , the paper layers were unwound and paper samples taken. These samples were put in hermetically sealed containers to prevent adsorption of atmospheric humidity, and sent to thermo-gravimetric analysis to assess their moisture content.

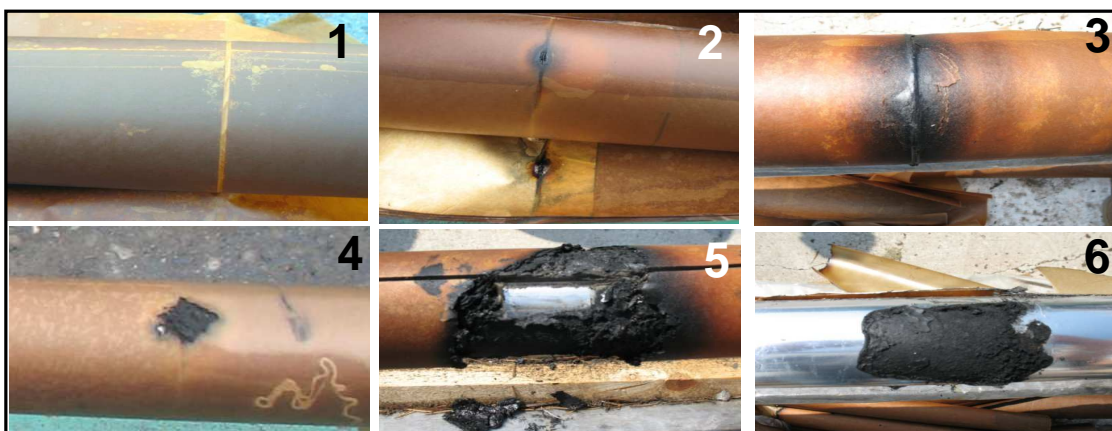


Fig. 3. Defective 400 kV OIP bushing core. Sequentially unwound layers of paper reveal carbonized pocket at approximately 60% of the bushing core length (counting from the bottom).

The outer layers were punctured at the gap between two adjacent paper sheets, visible in Fig. 3, first picture. This area was subjected to a higher stress, since the gap sandwiched between adjacent paper layers was filled with oil of nearly two fold lower dielectric strength than oil-saturated paper.

### ■ Typical location of the bushing-core fault

The bushing field-control foils ensure uniform distribution of dielectric stress along the surface of porcelain housing, but the radial distribution usually shows a slightly higher stress near the central tube, and sometimes near the flange [2].

The lower part of transformer bushing is immersed in the top oil that may attain and even exceed 90°C.

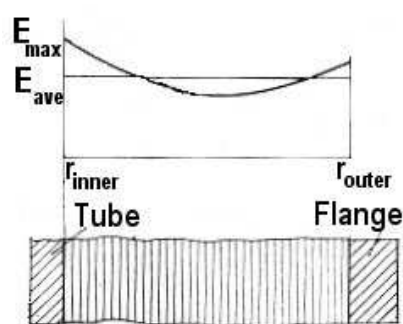


Fig. 1. Radial distribution of stress in the bushing core with the linear stress distribution along the porcelain-housing surface. Usually  $E_{\max} \leq 1,3 E_{\text{ave}}$ .

The high stress and high temperature in the wet-paper pocket accelerate degradation of cellulose, and water is one of decomposition products. A higher dielectric loss of the wet cellulose contributes to the local overheating and paper becomes carbonized after years of service [3]. Subsequently, the carbon short-circuits the inner paper layer, and the stress is shifted to the adjacent layers of the wet-paper pocket. Finally, the high potential is transferred to the healthy outer paper-layers that are punctured and break down under the excessive stress.

## Diagnostic procedures and their effectiveness

### ■ Moisture in paper assessment

The thermo-gravimetric test consists in putting the paper sample on a precision scale and heating under vacuum. As the paper temperature increases water evaporates and the sample weight decreases. A graph of the temperature and weight reveals the amount of evaporated water in the temperature range of approximately 100 °C. In such a way the water content in the paper sample can be determined. Subsequent heating results in evaporation of oil chemical components and finally in cellulose burning.

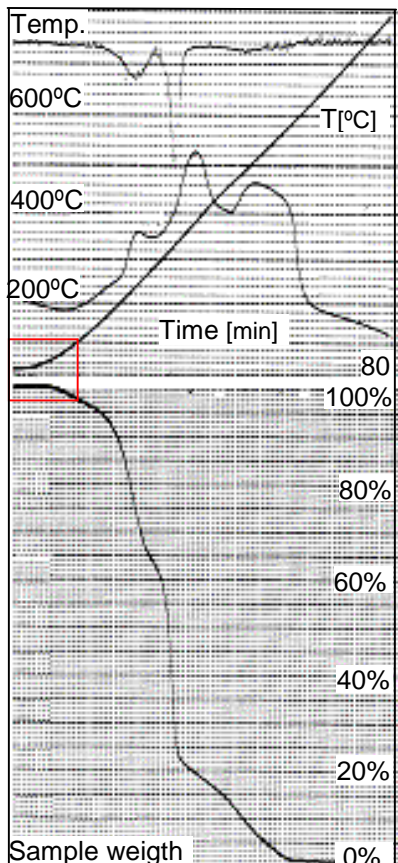


Fig. 4. Thermo-gravimetric record of paper sample taken from the bushing core close to the inner tube.

Although not very accurate, but water content in paper can be assessed by measuring the reduction of sample weight at 100°C (lower graph). The reading indicates a few percent (close to 5%) of water content in paper. This is a rather high value for bushing core, but not impossible considering the production of water due to the thermal decomposition of cellulose.

The thermo-gravimetric method is not intended to measure water content in paper, but to analyze evaporation (lower curve in upper graph) and evaporation rate (upper curve in upper graph) of oil chemical component at the temperature increasing up to 800°C in 80 minutes.

In consequence data read within 100°C range (marked by the rectangle) are not precise enough for quantitative determination, but provide indication of a rather high moisture content in paper sample taken in vicinity of the bushing inner-tube.

### ■ Bushing condition assessment based on dielectric polarization characteristics

Ingress of moisture to the bushing through a leaky seal affects the whole volume of cellulose. This can be detected by measurement of the bushing capacitance and dielectric-loss factor frequency-characteristic.

To interpret the recorded characteristic the bushing insulation is modeled by a combination of series and parallel RC two-poles [4]. Their respective elements reflect dielectric loss and conductive loss of paper-oil insulation. The model-predicted characteristics can be matched to the measured ones, and cellulose degradation can be revealed in the low-frequency range of C and  $\tan\delta$  characteristic.

Such characteristic can be measured directly with the aid of specialized instrument [5], or derived from the depolarization current records [6].

## ■ Polarization and depolarization current measurement

The bushing depolarization-current was recorded for one hour to assess the moisture content of a few 110 kV transformer-bushings removed from service. Different types of OIP type bushings were examined to gain practical experience in the measuring technique and analysis of the recorded depolarization current.

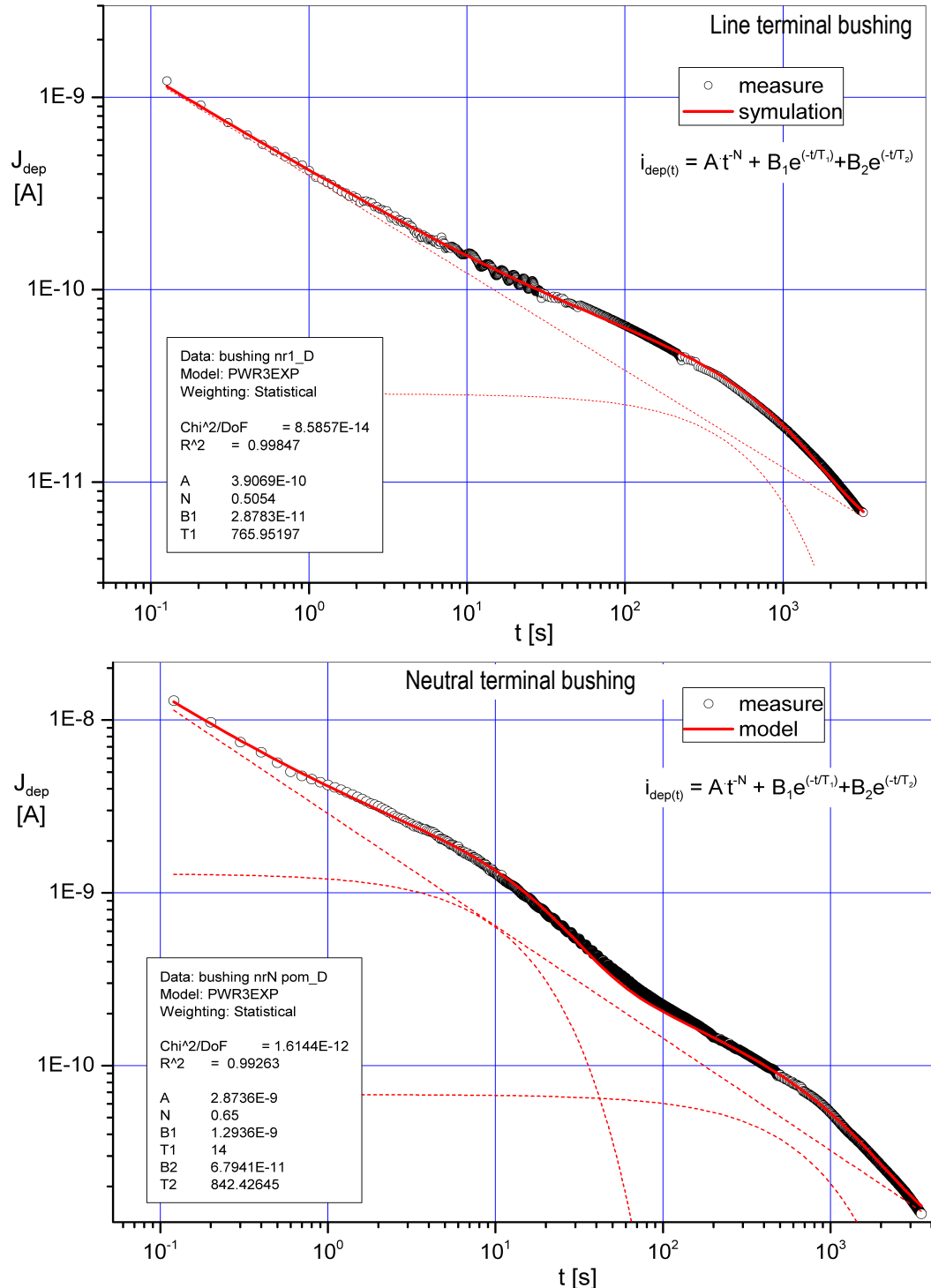


Fig. 5. Depolarization current recorded on the line-terminal (upper graph), and neutral-terminal (lower graph) bushings during one hour.

Curve-fitting algorithm was implemented to derive exponential components of the recorded current  $B \cdot e^{-t/T}$ , as well as the direct current  $i = A \cdot t^N$  that flows through the insulation conductance. With the known direct-current parameters: A and N, time-constant  $T_n$  of each exponential component n and its respective magnitude  $B_n$ , the insulation resistance R and moisture in cellulose was determined.

The parameters A, N, B1, T1, B2, T2 derived from of the depolarization current record were compared to the respective parameters of reference cellulose-samples conditioned and analyzed in the laboratory. Moisture content in bushing insulation was assessed at 1.1% to 1.5%.

The neutral-terminal bushing revealed a short time constant  $T_1=14$ s of the depolarization current. This must have been caused by relaxation of the space charge in an empty space within the insulation, which was left after a significant oil leak from the bushing.

The long time constant  $T_1=766$  s of the line terminal bushing and  $T_2=842$  s of the neutral-terminal bushing are characteristic to the low moisture content in cellulose.

### ■■ Frequency characteristic of C and $\tan \delta$ measurements

As a cross-check, the same bushings were examined by C-tan $\delta$  bridge that operates in frequency range from 1 mHz to 100 Hz, at the test voltage regulated up to 200 V [7].

Moisture content derived from the measured frequency-characteristics was close enough to the value obtained from depolarization current. However, the measuring uncertainty of the frequency-domain measurements was considerably larger, since the examined 110 kV bushing capacitance was small (130 to 160 pF) and the bridge test voltage of 200 V was 25 fold smaller than 5 kV direct-voltage used to measure depolarization current.

The insulation conductivity was also measured with a higher accuracy at 5 kV direct-voltage.

### Bushing-insulation thermal-model based on $\tan \delta$ measured as a function of voltage and frequency

Capacitance and dielectric-loss factor of three 400 kV bushings installed on a large power-transformer were measured at power frequency using a conventional low-voltage bridge. The bridge readings  $C=1,25 \div 1,36$  nF and  $\tan \delta=0.25 \div 0.35$  % indicated a low moisture content and good technical condition of bushings' insulation. However, phase A bushing has developed a slight oil leak, and this observation prompted a more advanced investigation of C and tan $\delta$ . These were measured as a function of voltage and frequency using a specialized bridge [8].

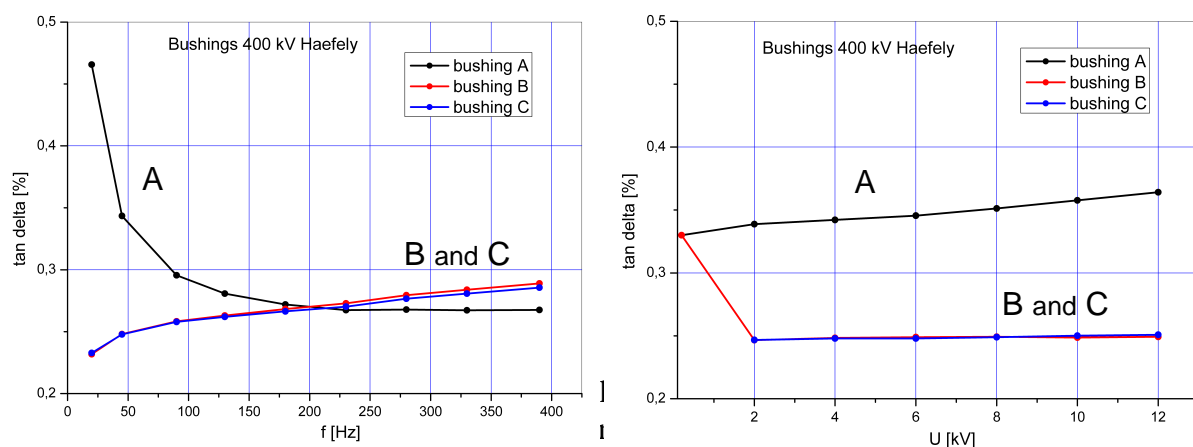


Fig. 7. Dielectric loss factor  $\tan \delta$  of three-phase 400 kV bushings measured as a function of frequency and test voltage.

A higher  $\tan\delta$  measured in the low-frequency range, and also at the increased test voltage suggested ingress of moisture to the phase A bushing. To confirm this finding the polarization  $i_{pol}$  and depolarization  $i_{dep}$  current was recorded, as well as the direct-current  $i_R$  flowing through the conductance of bushing core was derived.

$$\sigma \cong \frac{\epsilon_0}{U_{pol} \cdot C_o} [i_{pol}(t_{max}) - i_{dep}(t_{max})] = \frac{\epsilon_0 \cdot i_R}{U_{pol} \cdot C_o} \quad 1)$$

for bushing A:  $U_{pol} = 2000$  V,  $I_R \approx 7.6$  nA,  $\sigma \approx 0.09$  pS/m.

Fig. 6. Polarization  $i_{pol}$  and depolarization  $i_{dep}$  current recorded on three 400 kV bushings.

The current  $i_R$  that flows through the bushing core insulation and its conductivity  $\sigma$  was derived from the  $i_{pol}$  and  $i_{dep}$  characteristic, and from the bushing geometric capacitance  $C_o$ .

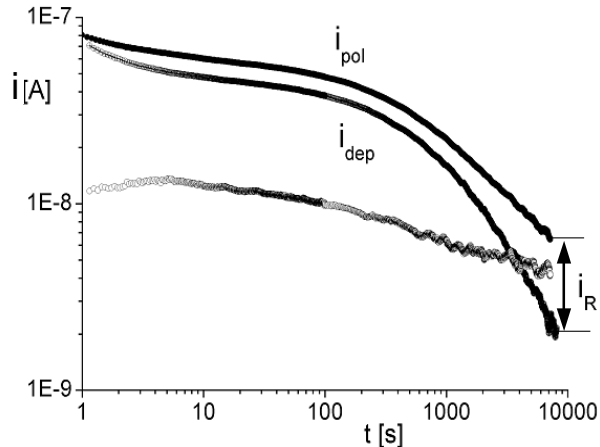


Table 1.  
DC leakage current, capacitance, conductivity and moisture content of the 400 kV bushings

Bushing #	Temperature [°C]	$i_R$ [nA]	$C_{bushing}$ [nC]	$\sigma$ [pS/m.]	$H_2O$ content [%]
A	20	7.6	1.36	0.09	2.2
B	26	4.4	1.25	0.05	1.7
C	24	5.0	1.25	0.06	1.7

The calculated moisture content in three bushing insulation, shown in Table 1, should be analyzed taking into account the temperature distribution within the bushing core.

In contrast to the transformer insulation that is mainly heated by the load loss, the HV bushing core is heated by the dielectric loss in cellulose. The latter increases with the water content in cellulose, its ageing and the ambient temperature. For instance, at the bushing porcelain-housing temperature of 35–40 °C and  $\tan\delta = 0.6\text{--}0.8$  %, the bushing core temperature may attain 85–95 °C, and wet cellulose starts to degrade at such temperature. The bushing core may attain an even higher temperature if the housing is exposed to an intense sunshine. At approximately 120 °C bubble effect may develop that leads to breakdown of paper insulation between adjacent aluminum layers.

Early thermal models [9, 10] developed for lower-voltage bushings did not account for the core heating by dielectric loss, but assumed the transformer-top oil as the main heat source. However, these models are still useful to calculate the rate of natural heat removal by ambient air.

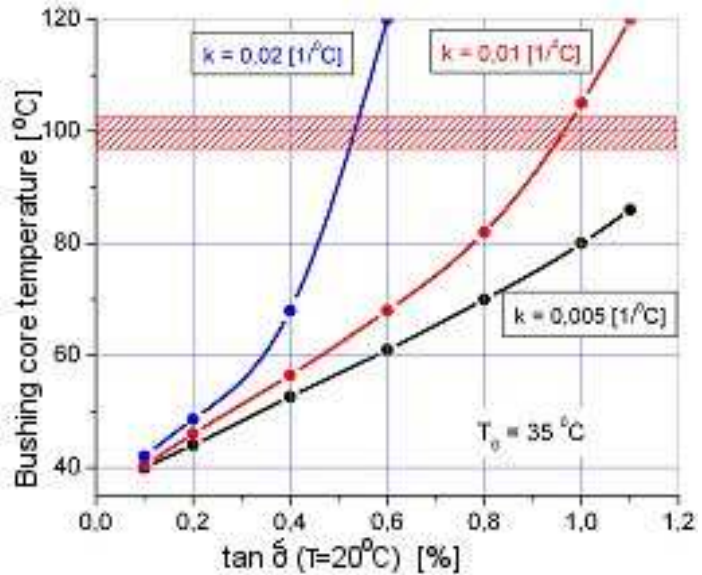
Contemporary thermal model of 400 kV and 800 kV class bushings includes the heat production by the dielectric loss. This model shows that the highest temperature develops at the inner layer of paper and at approximately 60% of the core length from the lower end. The temperature dependence of  $\tan\delta$  assumed in this model is given by:

$$\tan\delta(T) = \tan\delta(20^\circ\text{C}) \cdot \exp[k \cdot (T - 20^\circ\text{C})]$$

2)

where:  $k$  ranges between  $0.005[1/\text{ }^\circ\text{C}]$  and  $0.025[1/\text{ }^\circ\text{C}]$ , depending on the cellulose water content and ageing.

Fig. 9. The highest temperature inside the bushing core derived from the thermal model for the dielectric loss factor  $\tan\delta$  ranging from 0.01% to 1.2%, at the porcelain housing temperature  $T_0=35^\circ\text{C}$ , for the parameter  $k=0.005$ ; 0.01 and 0.02 that increases with the cellulose water-content and ageing ,



Although not yet confirmed by temperature measurements inside the bushing core, the thermal model indicates a real possibility of thermal breakdown of time-aged bushings with high moisture-content. The model predicted spot of the highest temperature coincides with the breakdown location of several bushings, observed at the post-mortem examination of failed units.

### Monitoring of alternating-current that leaks through the bushing

The concept of monitoring the sum of leakage current measured on three-phase bushings has been known and employed for years [11, 12]. This simple device indicates an asymmetry of the leakage current drawn from the compared bushings. The leakage-current sum plotted as a function of time reveals three possible outcomes: perfect symmetry, stable asymmetry or increasing asymmetry. In the latter case, the transformer is switched off, and bushings' capacitance and dielectric-loss factor are measured by a portable C-tan $\delta$  bridge that operates at  $\sim 12$  kV power-frequency test voltage [13]. However, only some insulation faults of say 800 kV or 400 kV class bushings can be detected at such voltage level.

A bushing monitoring system based on comparison of the leakage current recorded and compared to the current measured in units connected to the same phase, but in different transformers was developed and presented at 2008 Transformer Committee colloquium in Bruges [14]. This monitoring system is largely immune to perturbations that hamper operation of the circuit that displays the sum of three-phase bushing-leakage currents. However, a noticeable change of the leakage current reveals an advanced stage of the bushing insulation fault. Such monitoring system provides a warning signal that precedes an oncoming bushing explosion, but cannot reveal an early stage of the fault development.

### Partial discharge measurements

As measurement of C and tan $\delta$  at power frequency cannot detect early stages of the oncoming fault, the detection of partial discharges that accompany cellulose degradation under high stress may be considered as one of the promising diagnostic methods. However, the partial discharge level in a new HV bushing has to be lower than 10 pC (some specifications require a few pC) [15]. Partial discharges at such low level can be measured in a specialized HV laboratory, equipped with the electromagnetic shield and the test-voltage supply free from partial discharges.

HV power transformer in service may indicate partial discharges that largely exceed 100 pC, and they mask much smaller discharges originated from the bushing. An attempt to filter out the perturbations that prevail on transformers in substations has been made, and an advanced digital processing of partial discharges measured on bushings in service gives promising results [16].

### ■ Partial discharge between to adjacent foils in the bushing core

Breakdown of paper insulation between the adjacent aluminum foils occurs at the sine-voltage peak that may attain  $4\text{kV}_{\text{peak}}$  in 400 kV rated-voltage bushing. Capacitance of such insulation can be estimated as:

$$C = \frac{2\pi\epsilon_0\epsilon_r \cdot \ell}{\ln \frac{r_{\text{out}}}{r_{\text{in}}}} = 44\text{nF}, \quad 3)$$

where: the aluminum foil length  $\ell=4\text{ m}$ , inner foil radius  $r_{\text{in}}=0.098\text{ m}$ , the outer foil radius  $r_{\text{out}}=0.1\text{m}$ , oil-impregnated paper dielectric-constant  $\epsilon_r \approx 4$ . The charge stored in this capacitance  $Q=C \cdot U=176\text{ }\mu\text{C}$ .

Two concentric foils form co-axial transmission line of the characteristic impedance

$$Z = \frac{1}{2\pi} \cdot \sqrt{\frac{\mu_0}{\epsilon_0\epsilon_r}} \cdot \ln \frac{r_{\text{out}}}{r_{\text{in}}} = 0.6\Omega \quad 4)$$

Short-circuit current in the middle of this line is given by:

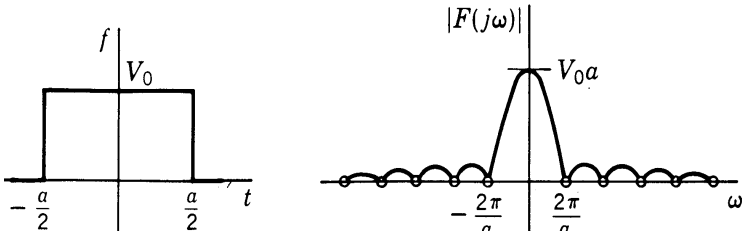
$$I = \frac{U}{Z} = 6.67\text{ kA}.$$

Duration of the current impulse  $\tau=2 \cdot t_p$ ; where:  $t_p$  the line transit time given by the pulse propagation rate  $v$  and the line length  $\ell/2$

$$v = \frac{c_0}{\sqrt{\epsilon_r}} = 200 \frac{\text{m}}{\mu\text{s}}; t_p = \frac{\ell}{2} \cdot v = 10\text{ ns}; \text{ and } \tau = 2 \cdot t_p = 20\text{ ns} \quad 5)$$

The discharge current waveform approaches rectangular pulse, and its spectrum is shown in Fig. 10.

Fig. 10. Rectangular impulse of the width  $\tau=20\text{ ns}$  has spectral components that stretch to  $\sim 50\text{ MHz}$ .



In reality, the discharge-current waveform deviates from rectangle, since the spark-channel resistance drops from an initial high value to a fraction of one ohm in a finite time. In consequence, the current impulse front is rounded off and the spectral harmonics are reduced at somewhat lower frequency. Nevertheless, the partial discharges that originate inside the bushing have spectral components extended to a much higher frequency than discharges coming from the transformer winding. The winding impedance behaves as a low-pass filter and attenuates higher frequency components of discharges that have to pass through the winding before they reach the bushing.

### ■ Detection of partial discharges based on electromagnetic radiation

A short-wave receiver that can be tuned within the frequency range from 20 MHz to 50 MHz will be able to detect partial-discharge electro-magnetic field radiated by 400 kV bushing. Such receiver can be mounted on an insulating rod and brought close to the bushings of transformer in service. Alternatively, the antenna can be installed in vicinity of HV bushing and serve as part of monitoring system. This concept to detect partial

discharges by measuring the radiated high-frequency electromagnetic field was pioneered by Dr. Eberhard Lemke, who designed his Lemke probe in 1970<sup>ies</sup> [17].

Fig. 11. "Lemke probe" detector of electromagnetic field radiated by partial-discharges in HV equipment.

This probe operates in frequency range of ~2 MHz, and can detect e.g. discharges in medium voltage cable joints. However, the probe frequency-range shall be at least ten times higher to detect partial discharges in HV bushing.



## Conclusions

1. In-service faults of transformer bushings of 220 kV and 400 kV voltage class become more frequent as these bushings approach the end of their service life, but simultaneous replacement of all older units is difficult and not justified economically. A bushing condition-assessment method is required to reveal early stages of the oncoming fault.
2. The standardized measurement of bushing capacitance C and dielectric-loss factor  $\tan\delta$  using the conventional, low-voltage bridge that operates at power frequency is not sensitive enough to detect the initial stage of bushing fault development. This technique can be enhanced by recording frequency characteristic of C and  $\tan\delta$ , as well as their voltage dependence.
3. Effectiveness of such diagnostic is satisfactory in the case of moisture ingress into the bushing housing and subsequent penetration into the whole volume of bushing core. However, experimental evidence indicates frequent faults that originate from a small pocket of cellulose, located at the inner radius of the core at approximately 60 % of the core length (from the bottom end).
4. Such small pocket of degraded cellulose cannot be detected by an increase of C and  $\tan\delta$  measured on the whole core, since these are integral quantities, averaged over the stressed core volume. Appearance of partial discharges indicates the localized fault that initially affects only one layer of paper insulation between adjacent foil shields. However, such discharges are much smaller than the partial discharges in transformer insulation, which mask the minute signals from inside the bushing.
5. Partial discharges in the bushing core must have spectral components that extend to a much higher frequency than discharges inside transformer windings, measured at the bushing capacitive tap. Reception of high frequency signals filtered out from the whole partial discharge spectrum is considered a promising method to detect the bushing internal fault at its early stage.

## References:

1. Abdollall, K., Vandermaar, A.J., "**Effects of Moisture on Power Factor of Oil/Paper Insulation**", 2006 Annual Report Conference on Electrical Insulation and Dielectric Phenomena, IEEE 1-4244-0547-5/06.
2. Kapeller, H., "**Recent Forms of Execution of 380 kV Transformer Bushings**", CIGRE 1958, Paris, paper #126.
3. Giaro, J. A., "**A study of the capacitive network and a generalized method of calculation of capacitor bushing for high-voltage cable**", CIGRE, Paris, 1952.
4. Houhanessian, V., D., Zaengl, W., S., "**Application of relaxation current measurements to on-site diagnosis of power transformers**", IEEE Conference on Electrical Insulation and Dielectric Phenomena, Minneapolis, October 19-22, 1997.

5. Kaul, G., Plath, R., Kalkner, W., "**Development of a Computerized Loss Factor Measurement System for Different Frequencies, Including 0.1 Hz and 50/60 Hz**", 8th ISH, Yokohama, 1993, paper 56.04
6. "**PDC-Analyzer-1MOD, Electrical Insulation Diagnostic System**" Alff Engineering pamphlet 2007, ([www.alff-engineering.ch/analyser.htm](http://www.alff-engineering.ch/analyser.htm)).
7. "**IDA 200 Insulation Diagnostic System**", pamphlet of Programma Electric, Taby, Sweden, 2006.
8. "**C-tan $\delta$  bridge model CPC100+TD1**" pamphlet of Omicron Inc., Klaus, Austria.
9. Hebert, P.P., Steed, R.C., "**A High Voltage Bushing Thermal Performance Model**", IEEE Trans. Vol. PAS-97, Nr. 6, Nov/Dec 1978, p. 2219-2224.
10. McNutt, W.J., Easley, J.K., "**Mathematical Modeling – A Basis for Bushing Loading Guide**", IEEE Trans. Vol. PAS-97, Nr. 6, Nov/Dec 1978, p. 2393-2404.
11. Lahmann, M. F., Walter, W., Guggenberg, P.A., "**Experience with Application of Sum Current Method to On-Line Diagnostics of High-Voltage Bushings..**", Sixty-Fifth Annual International Conference of Doble Clients, 1998, page 3-5.1.
12. Svi, P., Smekalov, V., "**Bushing Insulation Monitoring in the Course of Operation**", CIGRE 1996, Paris, paper #12-106.
13. Malewski, R., Kobi, R., Kopaczynski, J., Lemke, E., Werelius, P. "**Instruments for HV Insulation Testing in Substations**", CIGRE 2000, paper #12/33-06.
14. Picher, P., Rajotte, C., "**Field Experience with on-line Bushing Diagnostic to improve Transformer Reliability**", CIGRE SC A2 and D1 Joint Colloquium on Power Transformers, October 7-12, 2007, Bruges
15. "**Insulated Bushings for Alternating Voltages above 1000V**". IEC 60137, Edition 6.0, 2008-07.
16. Plath, R., "**MPD 600 Partial Discharge Analysis System**", Omicron mtronix technology, Omicron pamphlet, Klaus, Austria, 2008.
17. "**HV Diagnostics**", Lemke Diagnostics AG pamphlet, Volkersdorf, Germany, 2006.